Earthquakes and Structures, *Vol. 15, No. 1 (2018) 81-95*
DOI: https://doi.org/10.12989/eas.2018.15.1.081

Methods of analysis for buildings with uni-axial and bi-axial asymmetry in regions of lower seismicity

Elisa Lumantarna[*1,3], Nelson Lam[2,3a] and John Wilson[2,3a]

[1]*Department of Infrastructure Engineering, The University of Melbourne, Parkville 3030, Victoria, Australia*
[2]*Swinburne University of Technology, Sarawak Campus, Kuching, Sarawak, Malaysia*
[3]*Bushfire and Natural Hazards Cooperative Research Centre, Melbourne Australia*

(Received December 11, 2017, Revised April 9, 2018, Accepted April 10, 2018)

Abstract. Most buildings feature core walls (and shear walls) that are placed eccentrically within the building to fulfil architectural requirements. Contemporary earthquake design standards require three dimensional (3D) dynamic analysis to be undertaken to analyse the imposed seismic actions on this type of buildings. A static method of analysis is always appealing to design practitioners because results from the analysis can always be evaluated independently by manual calculation techniques for quality control purposes. However, the equivalent static analysis method (also known as the lateral load method) which involves application of an equivalent static load at a certain distance from the center of mass of the buildings can generate results that contradict with results from dynamic analysis. In this paper the Generalised Force Method of analysis has been introduced for multi-storey buildings. Algebraic expressions have been derived to provide estimates for the edge displacement ratio taking into account the effects of dynamic torsional actions. The Generalised Force Method which is based on static principles has been shown to be able to make accurate estimates of torsional actions in seismic conditions. The method is illustrated by examples of two multi-storey buildings. Importantly, the black box syndrome of a 3D dynamic analysis of the building can be circumvented.

Keywords: generalised force method; static analysis method; plan irregularity; torsion

1. Introduction

Many multi-storey buildings feature core walls (and shear walls) that are asymmetrically disposed within the floor plan of the building. Consequently, the centre of stiffness can be significantly offset from the centre of mass of the building thereby raising concern over the generation of high torsional actions in seismic conditions. Plan irregularities in the building are common, and more so in regions of low-to-moderate seismicity, in spite of the well-publicised undesirable implications from the structural performance perspectives (e.g., Ceci *et al.* 2010, Westenek *et al.* 2013, Ferraioli 2015).

Research that is focused on seismically induced torsional actions in buildings commenced in the early 1980's. Early investigations were mainly about developing a quasi-static analytical approach to design featuring the use of a so called "dynamic eccentricity", or "effective eccentricity", in covering for a projected amount of torsional actions in the building based on results from dynamic analyses assuming linear elastic behaviour (e.g., Tscinias and Hutchinson 1981, Dempsey and Tso 1982, Chandler and Hutchinson 1986). More recent studies took into account post-elastic non-linear behaviour (e.g., Chandler and Duan 1997, Dimova and Alashki 2003, Sommer and Bachman 2005, Stathopoulos and Anagnostopoulos 2010). The objectives of the latter type of investigations were to assess the adequacy of provisions in certain targeted clauses that were stipulated by major codes of practice at the time. There have also been publications to promote, or evaluate, certain analytical methodologies (e.g., Poursha *et al.* 2014, Cimellaro *et al.* 2014, Magliulo *et al.* 2012, D'Ambrisi *et al.* 2009). The most comprehensive, and detailed, literature review on the topic of torsional actions in buildings in seismic conditions by Anagnostopoulos *et al.* (2015) reported that some 600-700 technical articles had been published. However, there is a lack of consensus over how best to incorporate the research findings into codified provisions. Perceived contradictions in findings reported in the literature have added to the challenges. Contemporary seismic design standards typically stipulate that 3D dynamic analysis of the building is to be performed. The following is a list of examples: Eurocode 8 (EN 1998-1 2004); FEMA 450-1 (Building Seismic Safety Council 2003); FEMA 356 (ASCE 2000); AS1170.4:2007 (Standards Australia 2007). The proliferation of commercial software with 3D dynamic analysis capability also means that emphasis has been shifted towards placing reliance on results from 3D dynamic analysis as opposed to the use of equations for determining a certain design eccentricity that have been derived from research (other than imposing a prescribed amount of torsional moment associated with the so called "accidental" eccentricity which is additive to the computed dynamic actions).

The authors are of the opinion that the current practice of placing reliance on the use of the computer to quantify

∗Corresponding author, Lecturer
E-mail: elu@unimelb.edu.au
[a]Professor

ISSN: 2092-7614 (Print), 2092-7622 (Online)

design seismic actions is not entirely satisfactory given that no known calculation method exists to allow designers to independently evaluate results from the 3D dynamic analysis of a structure. It should be recognised that static analysis has the intrinsic merit of allowing independent checks to be undertaken by a competent structural design engineer. The Generalised Force Method (GFM) was first introduced as a static analysis procedure to provide estimates of seismic actions in low rise, or medium rise, buildings to approximate results from dynamic analysis. GFM was initially restricted to the 2D analysis of buildings with symmetrical floor plans, and have been extended to the analysis of buildings with floor plans featuring uni-axial asymmetry (Lam *et al.* 2016). These earlier versions of GFM will be introduced in Sections 2 and 3 for the benefits of readers who have not been informed of the developed techniques.

GFM is developed further in this paper to handle floor plans featuring bi-axial asymmetry. Design expressions have been developed to take into account dynamic torsional amplification forming part of the static analysis procedure (Section 4). The practical application of the newly introduced analytical procedure is illustrated by working through examples (Section 5). In view of the limited ductile behaviour of the considered building systems in a low-to-moderate seismicity environment linearly elastic behaviour has been assumed to reduce the number of variables to be handled in the parametric study. Post-elastic behaviour is to be taken into account by the structural modification (or behaviour) factor which a topic in its own right and is not within the scope of this article. The effects of higher modes which cannot be ignored in high-rise buildings (taller than 30 m or so in this context) are also outside the scope of this article as the subject matter is treated elsewhere (Lumantarna *et al.* 2017).

2. Generalised force method (GFM) for torsionally balanced (TB) building

The original version of the Generalised Force Method (GFM) which is only suited to the analysis of low-rise, or medium-rise, torsionally balanced (TB) multi-storey buildings is introduced briefly in this section. Further details can be found in Lam *et al.* (2016).

First, an equivalent static analysis is undertaken in accordance with standard seismic design procedures; refer AS 1170.4:2007 (Standards Australia 2007) or Eurocode 8 (EN 1998-1 2004). The deflection value at each floor is to be obtained by standard structural analysis techniques. Refer the schematic diagram of Fig. 1. The multi-storey building response is idealised into a single-degree-of-freedom (SDOF) system. The behaviour of the building in response to the applied lateral force is characterised by the effective displacement (δ_{eff}) and the effective mass (m_{eff}) which can be calculated using Eqs. (1) and (2), respectively.

$$\delta_{eff} = \frac{\sum m_i \delta_i^2}{\sum m_i \delta_i} \tag{1}$$

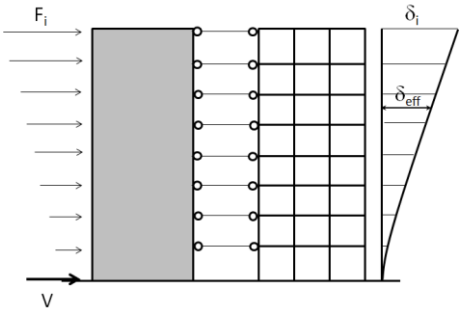

Fig. 1 Displacement values based on equivalent static analysis

$$m_{eff} = \frac{(\sum m_i \delta_i)^2}{\sum m_i \delta_i^2} \tag{2}$$

where, m_i and δ_i are the mass and displacement of floor *i*, respectively.

The capacity diagram is then plotted in the acceleration vs displacement format (Fig. 2(a)), in which the effective acceleration (a_{eff}) is defined by Eq. (3).

$$a_{eff} = \frac{V}{m_{eff}} \tag{3}$$

where, V is the horizontal equivalent static shear force.

The effective stiffness (k_{eff} and effective natural period (T_{eff}) of the buildings are accordingly calculated using Eqs. (4) and (5).

$$k_{eff} = \frac{V}{\delta_{eff}} \tag{4}$$

$$T_{eff} = 2\pi \sqrt{\frac{m_{eff}}{k_{eff}}} \tag{5}$$

The capacity diagram is then superposed onto the demand diagram in the acceleration-displacement response spectrum format (the ADRS diagram) as shown schematically in Fig. 2(b) to determine the performance point through which the seismically induced displacement demand of the building (δ^*_{eff}) is identified. The use of the ADRS diagram in lieu of the response spectrum representing seismic actions has been introduced and illustrated in Wilson and Lam (2006). The displacement demand (δ^*_{eff}) that has been identified can be used for calculating the displacement demand values (δ^*_i) at individual floor levels based on Eq. (6a) as illustrated in Fig. 3

$$\delta^*_i = \frac{\delta^*_{eff}}{\delta_{eff}} \delta_i \tag{6a}$$

and the seismic inertia forces at each floor level can be adjusted based on Eq. (6b)

$$F^*_i = \frac{\delta^*_{eff}}{\delta_{eff}} F_i \tag{6b}$$

where δ_i and F_i are displacement and inertia force values at floor level *i* from equivalent static analysis, δ_{eff} is the

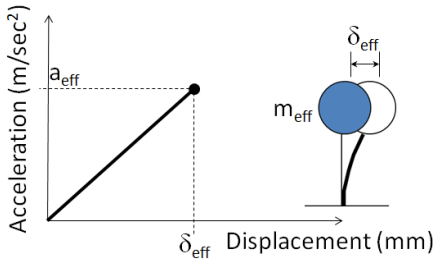

(a)

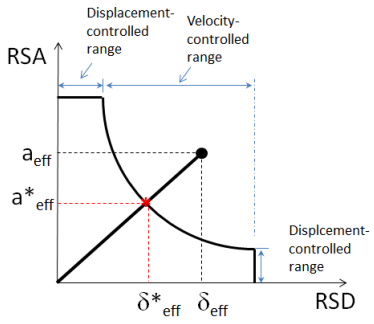

(b)

Fig. 2 (a) Capacity diagram in the acceleration vs displacement format, (b) Superposition of the capacity and demand diagrams

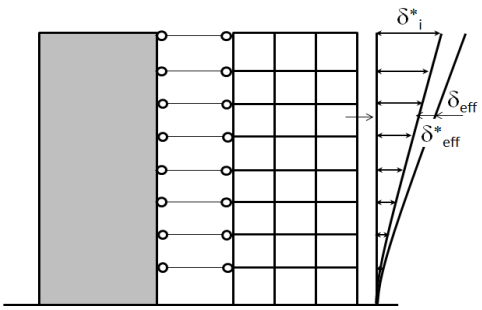

Fig. 3 The displacement demand values of the TB buildings

corresponding effective displacement, and δ_i^* and F_i^* are the revised displacements and inertia forces at level *i*.

The storey shear (V_i^*) can then be found using Eq. (6c).

$$V_i^* = \sum_i^n F_i^* \tag{6c}$$

where *n* is the number of floor levels in the building.

The GFM method as described can be used to analyse the displacement demand behaviour of low to medium rise (TB) buildings of which higher modes effects are not significant.

3. GFM for multi-storey torsionally unbalanced (TU) buildings with uni-axial asymmetry

Uni-axial asymmetry in this context refers to floor plans of the building in which the center of rigidity CR is offset from the center of mass CM along one-axis only, and is the axis which is perpendicular to the direction of ground motion. When subject to lateral seismic action the building

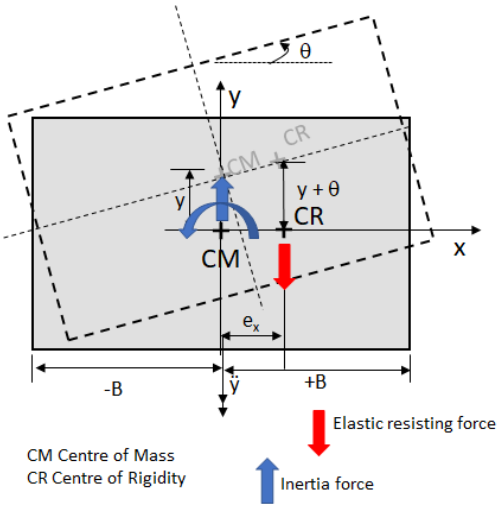

Fig. 4 Uni-axial asymmetry single-storey building model

will translate (in one direction) and rotate causing the highest displacement demand at the edges. Plan irregularities which commonly exist in multi-storey buildings are often resulted from lateral load resisting elements (e.g., cores or shear walls) that are eccentrically disposed within the floor plan of the building. The Generalised Force Analysis (GFM) which was introduced in Section 2 has been extended to account for torsional actions in buildings featuring uni-axial asymmetry (Lam *et al.* 2016). Details of the extension is summarised in this section.

A single-storey building model which is torsionally-unbalanced (TU) is used in Sections 3 and 4 to characterise the torsional response behaviour of the building. The building model is made up of a rigid diaphragm which is supported by lateral resisting elements that are disposed with uni-axial asymmetry (Fig. 4). Expressions to provide estimates of the maximum displacement demand at the edges of the building are then derived. The expressions can be applied on the storey displacements of multi-storey buildings based on the assumption that the torsional behaviour of the buildings can be represented by the single-storey building model. Hence the variations in the values of storey eccentricity and torsional stiffness were assumed to be insignificant and can be represented by a single value of eccentricity and torsional stiffness. The methodology to determine the eccentricity and torsional stiffness for multi-storey buildings have been described in Lam *et al.* (2016).

The torsional response behaviour of a torsionally unbalanced (TU) building with uni-axial asymmetry is governed by the following parameters:

i) e_x is the eccentricity perpendicular to the direction of motion:

$$e_x = \frac{\sum_i^n k_{y,i} x_i}{K_y} \tag{7a}$$

where, $k_{y,i}$ is the translational stiffness of the structural elements in the y-direction of motion and x_i is the distance from the structural elements to a reference point (e.g., the CM of the building).

ii) K_y is the translational stiffness in the *y*-direction of

motion

$$K_y = \sum_i^n k_{y,i} \tag{7b}$$

iii) K_θ is the torsional stiffness of the TU building

$$K_\theta = \sum_i^n k_{y,i}(x_i - e_x)^2 \tag{7c}$$

iv) M is the mass of the TU building; v) J is the torsional mass of inertia of the TU building ($= Mr^2$), where r is the mass radius of gyration; and vi) parameter "b" defined by

$$b = \sqrt{K_\theta / K_y} \tag{7d}$$

is used to represent the torsional stiffness properties of the TU building.

A uni-axial asymmetrical building model has two degree of freedoms (2DOFs): translation in the direction of motion y and rotation θ. The dynamic equations of equilibrium equation for the 2DOFs can be expressed in a matrix format as shown by Eq. (8).

$$\omega_x^2 \begin{bmatrix} 1 & e_{xr} \\ e_{xr} & b_r^2 + e_{xr}^2 \end{bmatrix} \begin{Bmatrix} y_r \\ \theta \end{Bmatrix} - \Omega_j^2 \begin{bmatrix} 1 & 0 \\ 0 & 1 \end{bmatrix} \begin{Bmatrix} y_r \\ \theta \end{Bmatrix} = \begin{Bmatrix} 0 \\ 0 \end{Bmatrix} \tag{8}$$

where, ω_x is the translational natural angular velocity of the uncoupled mode of vibration and Ω_j is the natural angular velocity of the coupled modes of vibration. b_r, y_r and e_{xr} are b, y and e_x that are normalised with respect to radius of gyration (r).

Letting $\lambda_j^2 = \frac{\Omega_j^2}{\omega_j^2}$, the two eigenvalues solution for Eq. (8) is given by

$$\lambda_j^2 = \frac{1 + (b_r^2 + e_{xr}^2)}{2} \pm \sqrt{\left[\frac{1 - (b_r^2 + e_{xr}^2)}{2}\right]^2 + e_{xr}^2} \tag{9}$$

Solution to the dynamic equation of equilibrium Eq. (8) can be represented by the two eigenvalues: λ_1 defining the first coupled natural angular velocity with value smaller than 1.0, and λ_2 defining the second coupled natural angular velocity with value greater than 1.0.

The corresponding eigenvectors defining the mode shapes can be represented by Eq. (10).

$$\begin{Bmatrix} y_{r,j} \\ \theta_j \end{Bmatrix} = \begin{Bmatrix} 1 \\ \left(\frac{\lambda_j^2 - 1}{e_{xr}}\right) \end{Bmatrix} \tag{10}$$

Given the eigenvalues and eigenvectors as defined by Eqs. (9) and (10) and the use of the well known SRSS combination rule, the maximum displacement at the edges of the building (Fig. 4) can be calculated using Eq. (11). The SRSS combination rule has been shown to be able to provide reasonably accurate estimates of the maximum displacement demand of TU buildings (Lumantarna *et al.* 2013).

$$y_{\pm B}(\max) = \sqrt{\sum_{j=1}^{2} \left(1 + \theta_j(\pm B_r)\right) \times PF_j \times RSD(T_j, \xi)} \tag{11}$$

where, y_{+B} is the maximum displacement at the stiff edge of the building, y_{-B} is the maximum displacement at the flexible edge of the building and B_r is the distance from the CM to the edge of the building, normalised with respect to r. The flexible edge of the building is defined herein as the edge that is furthest from the building CR whereas the stiff edge is the edge that is the closest to the CR of the building. $RSD(T_j, \xi)$ is the response spectral displacement value at the coupled modal period T_j of the building, and PF_j is the participation factor which can be calculated using Eq. (12).

$$\begin{aligned} PF_j &= \frac{\left\{1 \quad \frac{\lambda_j^2 - 1}{e_{xr}}\right\} \begin{bmatrix} 1 & 0 \\ 0 & 1 \end{bmatrix} \begin{Bmatrix} 1 \\ 0 \end{Bmatrix}}{\left\{1 \quad \frac{\lambda_j^2 - 1}{e_{xr}}\right\} \begin{bmatrix} 1 & 0 \\ 0 & 1 \end{bmatrix} \begin{Bmatrix} 1 \\ \frac{\lambda_j^2 - 1}{e_{xr}} \end{Bmatrix}} \\ &= \frac{1}{1 + \left(\frac{\lambda_j^2 - 1}{e_{xr}}\right)^2} = \frac{1}{1 + {\theta_j}^2} \end{aligned} \tag{12}$$

The maximum displacement demand of the TU building can be expressed in the form of the displacement ratio (δ/δ_o). δ is the maximum displacement of the TU building at the edges and δ_o is the maximum displacement of the equivalent torsionally balanced (TB) building. The displacement ratio is defined for the acceleration, velocity and displacement controlled conditions (as presented schematically in Fig. 5) and by Eqs. (13a)-(13c).

$$\frac{\delta}{\delta_0} = \frac{x_{\pm B}(\max)}{RSD(T, \xi)} = \sqrt{\sum_{j=1}^{2} \left[\frac{1 + \theta_j(\pm B_r)}{1 + \theta_j^2} \times \frac{1}{\lambda_j^2}\right]^2} \tag{13a}$$

for the acceleration-controlled conditions,

$$\frac{\delta}{\delta_0} = \frac{x_{\pm B}(\max)}{RSD(T, \xi)} = \sqrt{\sum_{j=1}^{2} \left[\frac{1 + \theta_j(\pm B_r)}{1 + \theta_j^2} \times \frac{1}{\lambda_j}\right]^2} \tag{13b}$$

for the velocity-controlled conditions, and

$$\frac{\delta}{\delta_0} = \frac{x_{\pm B}(\max)}{RSD(T, \xi)} = \sqrt{\sum_{j=1}^{2} \left[\frac{1 + \theta_j(\pm B_r)}{1 + \theta_j^2}\right]^2} \tag{13c}$$

for the displacement-controlled conditions.

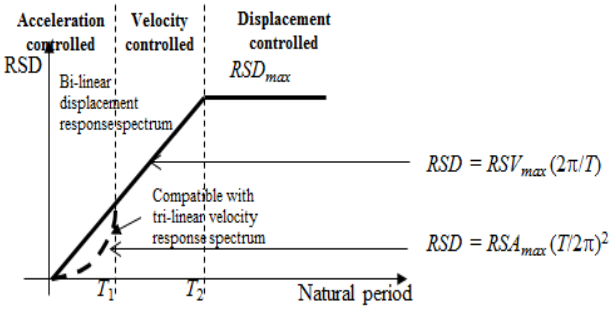

Fig. 5 Displacement response spectrum featuring acceleration-, velocity- and displacement-controlled region

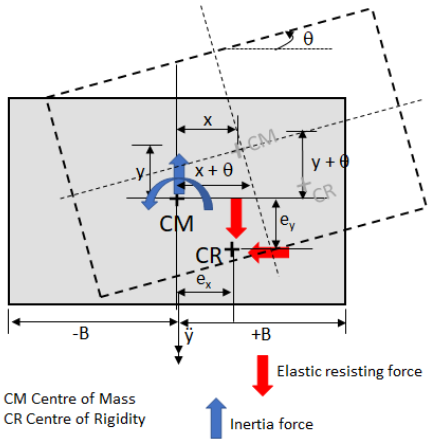

Fig. 6 Single-storey building model featuring bi-axial asymmetry

The displacement ratios as defined by Eqs. (13a)-(13c) can be used alongside the two-dimensional model of the TU building for estimating the maximum displacement demand at the edges.

4. GFM for multi-storey TU buildings with bi-axial asymmetry

GFM is extended further in this paper to handle buildings featuring bi-axial asymmetry. Expressions for estimating the maximum displacement demand at the edges of this very common type of buildings are derived in this section (based on single-storey building model idealisation in a manner similar to that described in Section 3).

4.1 Expressions for maximum displacement demand at the edges of the TU building

The single-storey building model featuring bi-axial asymmetry consists of a rigid diaphragm which is supported by a configuration of lateral load resisting elements which are eccentrically disposed within the floor plan of the building about both orthogonal axes as shown in Fig. 6. As a result, the building model possesses three degree of freedoms (3DOfs): translation in the direction which is orthogonal to the direction of motion x, translation in the direction of motion y, and rotation θ (Fig. 6). Uni-axial ground motion has been assumed to act along the y-direction of the building (as indicated in Fig. 6).

The dynamic equation of equilibrium for the 3DOFs can be defined by taking moment about the CM

$$M\ddot{x} + K_x\left(x + e_y\theta\right) = 0 \qquad \text{in the x-direction} \qquad (14a)$$

$$M\ddot{y} + K_y(y + e_x\theta) = 0 \qquad \text{in the y-direction} \qquad (14b)$$

$$J\ddot{\theta} + K_x\left(x + e_y\theta\right)e_y + K_y(y + e_x\theta)e_x + K_\theta\theta = 0 \qquad \text{in the } \theta\text{-direction} \qquad (14c)$$

where, M is the mass of the building, J is the torsional mass of inertia of the TU building ($= Mr^2$), K_y is the translational stiffness in the y-direction as defined by Eq. (7b), K_x is the translational stiffness in the x-direction of motion defined by

$$K_x = \sum_i^n k_{x,i} \qquad (15a)$$

where, $k_{x,i}$ is the translational stiffness of the structural elements in the *x*-direction of motion.

The model also features two eccentricities: e_x,which is the eccentricity in the direction perpendicular to the direction of the ground motion (Eq. (7a)); and e_y, which is the eccentricity in the direction parallel to the direction of the ground motion, defined by

$$e_y = \frac{\sum_i^m k_{x,i}y_i}{K_x} \qquad (15b)$$

where y_i is the distance from the structural elements to the CM of the building and K_θ is the torsional stiffness as defined by Eq. (15c) for TU building with bi-axial asymmetry.

$$K_\theta = \sum_i^n k_{y,i}(x_i - e_x)^2 + \sum_i^m k_{x,i}\left(y_i - e_y\right)^2 \qquad (15c)$$

As e_x contributes to the *y*-direction of motion (i.e., direction parallel to the direction of the ground motion), e_x is referred herein as the eccentricity in the *parallel* direction. Conversely, e_y is referred herein as the eccentricity in the *perpendicular* direction.

Dividing Eqs. (14a)-(14c) by M and r and letting $a = \frac{K_x}{K_y}$ results in Eqs. (16a)-(16c).

$$\ddot{x_r} + \omega_y^2\left(ax_r + ae_{yr}\theta\right) = 0 \qquad (16a)$$

where $\omega_y^2 = \frac{K_y}{M}$, $\ddot{x_r} = \frac{\ddot{x}}{r}$, $x_r = \frac{x}{r}$ and $e_{yr} = \frac{e_y}{r}$, Eq. (14b) can be re-written as

$$\ddot{y_r} + \omega_y^2(y_r + e_{xr}\theta) = 0 \qquad (16b)$$

where $\omega_y^2 = \frac{K_y}{M}$, $\ddot{y_r} = \frac{\ddot{y}}{r}$, $y_r = \frac{y}{r}$ and $e_{xr} = \frac{e_x}{r}$, and Eq. (14c) can be re-written as

$$\ddot{\theta} + \omega_y^2\left[ae_{yr}x_r + e_{xr}y_r + \left(ae_{yr}^2 + e_{xr}^2 + b_r^2\right)\theta\right] = 0 \qquad (16c)$$

where, $b^2 = \frac{K_\theta}{K_y}$ and $b_r = \frac{b}{r}$.

Expressing Eqs. (16a)-(16c) into the matrix format

$$\begin{bmatrix}1 & 0 & 0\\ 0 & 1 & 0\\ 0 & 0 & 1\end{bmatrix}\begin{Bmatrix}\ddot{x_r}\\ \ddot{y_r}\\ \ddot{\theta}\end{Bmatrix} + \omega_y^2\begin{bmatrix}a & 0 & ae_{yr}\\ 0 & 1 & e_{xr}\\ ae_{yr} & e_{xr} & ae_{yr}^2 + e_{xr}^2 + b_r^2\end{bmatrix}\begin{Bmatrix}x_r\\ y_r\\ \theta\end{Bmatrix} = \begin{Bmatrix}0\\ 0\\ 0\end{Bmatrix} \qquad (17)$$

Eigen-solutions to the dynamic equation of equilibrium can be represented as follows

$$\omega_y^2\begin{bmatrix}a & 0 & ae_{yr}\\ 0 & 1 & e_{xr}\\ ae_{yr} & e_{xr} & ae_{yr}^2 + e_{xr}^2 + b_r^2\end{bmatrix}\begin{Bmatrix}x_r\\ y_r\\ \theta\end{Bmatrix} - \Omega_j^2\begin{bmatrix}1 & 0 & 0\\ 0 & 1 & 0\\ 0 & 0 & 1\end{bmatrix}\begin{Bmatrix}x_r\\ y_r\\ \theta\end{Bmatrix} = \begin{Bmatrix}0\\ 0\\ 0\end{Bmatrix} \qquad (18)$$

where, Ω_j are the natural angular velocities of the coupled modes of vibration (i.e., the eigenvalues solution). Given that a single-storey building model with bi-axial asymmetry possesses 3DOFs, the building model features 3 coupled modes of vibration (i.e., 3 eigenvalues and 3 eigenvectors).

Letting $\lambda_j^2 = \frac{\Omega_j^2}{\omega_y^2}$ and re-arranging Eq. (18) results in Eq. (19).

$$\left\{\begin{bmatrix} a & 0 & ae_{yr} \\ 0 & 1 & e_{xr} \\ ae_{yr} & e_{xr} & ae_{yr}^2 + e_{xr}^2 + b_r^2 \end{bmatrix} - \lambda_j^2 \begin{bmatrix} 1 & 0 & 0 \\ 0 & 1 & 0 \\ 0 & 0 & 1 \end{bmatrix}\right\} \begin{Bmatrix} x_r \\ y_r \\ \theta \end{Bmatrix} = \begin{Bmatrix} 0 \\ 0 \\ 0 \end{Bmatrix} \quad (19)$$

To fulfil the conditions of dynamic equilibrium, condition expressed by Eq. (20) would need to be met.

$$det \begin{vmatrix} a - \lambda_j^2 & 0 & ae_{yr} \\ 0 & 1 - \lambda_j^2 & e_{xr} \\ ae_{yr} & e_{xr} & \left(ae_{yr}^2 + e_{xr}^2 + b_r^2\right) - \lambda_j^2 \end{vmatrix} = 0 \quad (20)$$

Solution for eigenvalues of λ_j^2 can be obtained by solving Eq. (20). Solution for the eigenvectors is accordingly obtained by solving Eq. (21).

$$\begin{bmatrix} a - \lambda_j^2 & 0 & ae_{yr} \\ 0 & 1 - \lambda_j^2 & e_{xr} \\ ae_{yr} & e_{xr} & \left(ae_{yr}^2 + e_{xr}^2 + b_r^2\right) - \lambda_j^2 \end{bmatrix} \begin{Bmatrix} x_{r,j} \\ y_{r,j} \\ \theta_j \end{Bmatrix} = \begin{Bmatrix} 0 \\ 0 \\ 0 \end{Bmatrix} \quad (21)$$

By letting $y_{r,j} = 1$

$$\theta_j = \frac{\lambda_j^2 - 1}{e_{xr}} \quad (21a)$$

and

$$x_{r,j} = \frac{e_{yr}}{e_{xr}} \left(\frac{a - a\lambda_j^2}{a - \lambda_j^2}\right) \quad (21b)$$

The maximum displacement of the TU building can be presented in the form of displacement ratio (δ/δ_o) where δ is the maximum displacement of the (TU) building at the edges and δ_o is the maximum displacement of the equivalent torsionally balanced (TB) building ($RSD(T_j, \xi)$). The displacement ratio can be calculated using Eqs. (22a)-(22c) for the acceleration, velocity and displacement-controlled conditions (as defined by the schematic diagram of Fig. 5).

$$\frac{\delta}{\delta_0} = \sqrt{\sum_{j=1}^{3} \left[\left(1 + \theta_j(\pm B_r)\right) PF_j \times \frac{1}{\lambda_j^2}\right]^2} \quad (22a)$$

for the acceleration-controlled conditions

$$\frac{\delta}{\delta_0} = \sqrt{\sum_{j=1}^{3} \left[\left(1 + \theta_j(\pm B_r)\right) PF_j \times \frac{1}{\lambda_j}\right]^2} \quad (22b)$$

for the velocity-controlled conditions, and

$$\frac{\delta}{\delta_0} = \sqrt{\sum_{j=1}^{3} \left[\left(1 + \theta_j(\pm B_r)\right) PF_j\right]^2} \quad (22c)$$

for the displacement-controlled conditions.

Where, PF_j is the participation factor that can be calculated using Eq. (23)

$$PF_j = \frac{[x_{r,j} \quad 1 \quad \theta] \begin{bmatrix} 1 & 0 & 0 \\ 0 & 1 & 0 \\ 0 & 0 & 1 \end{bmatrix} \begin{Bmatrix} 0 \\ 1 \\ 0 \end{Bmatrix}}{[x_{r,j} \quad 1 \quad \theta] \begin{bmatrix} 1 & 0 & 0 \\ 0 & 1 & 0 \\ 0 & 0 & 1 \end{bmatrix} \begin{Bmatrix} x_{r,j} \\ 1 \\ \theta_j \end{Bmatrix}} = \frac{1}{x_{r,j}^2 + y_{r,j}^2 + \theta_j^2} \quad (23a)$$

$$PF_j = \frac{1}{1 + \left(\frac{e_{yr}}{e_{xr}} \left(\frac{a - a\lambda_j^2}{a - \lambda_j^2}\right)\right)^2 + \theta_j^2} \quad (23b)$$

4.2 Parametric studies

Expressions that have been derived in Section 4.1 were employed in a parametric study for providing estimates of the displacement ratios for TU buildings with bi-axial asymmetry. Parameter *B* is defined as the offset of the edge of the building from its CM. The dimensionless parameter B_r is *B* normalised with respect to the mass radius of gyration *r*, and was kept constant at 1.8 in the parametric study to represent a rectangular floor plate with a very high aspect ratio. The other dimensionless parameter b_r which is used to characterise the torsional stiffness properties of the model has values varying in between 0.8 (representing a torsionally flexible building) and 1.6 (representing a torsionally stiff building). Results of the parametric studies are presented for the b_r values greater than 1.0 as the use of torsionally flexible building (b_r values less than 1.0) is discouraged in practice. The results for the b_r values of 0.8 and 1.0 are presented in the Appendix for readers to consult. The eccentricity in the *x*-direction (parallel direction) e_{xr} (normalised with respect to *r*) has values varying in the range: 0.1-0.9, whereas eccentricity in the *y*-direction (perpendicular direction) e_{yr} has values varying in the range: 0.05-0.6.

Single-storey building models with bi-axial asymmetry feature three coupled modes of vibrations. Values of the frequency ratios are plotted against b_r in Fig. 7. The values of the frequency ratios control the amount of modal rotation of the building as indicated by Eq. (21a). The values of the frequency ratios (characterising rotational behaviour) are not significantly affected by the values of eccentricity especially when the buildings are torsionally stiff (buildings with b_r greater than 1.0). As the torsional stiffness of the building increases, it becomes less sensitive to changes in the value of the eccentricity parameters. These behavioural trends have also been observed in TU buildings featuring uni-axial asymmetry (Lam *et al.* 2016). It is also noted that

values of λ_3 increases with increasing values of b_r indicating an increase in rotation contributed by the third mode of vibration. However, the third mode of vibration does not have significant contribution to the overall response behaviour of the building. Interestingly, values of frequency ratios becomes less sensitive to changes in the values of the torsional parameters in cases where eccentricity in the direction perpendicular to the direction of motion (e_{xr}) is large.

The maximum edge displacement demand (δ) of the TU building models can be obtained by the use of Eqs. (21)-(23) provided that the frequency ratios have been solved. These displacement values are also presented in the form of charts showing the displacement ratios (δ/δ_0) for K_x/K_y=0.5 (Figs. 8-11). These charts may be used in lieu of the equations in cases where the value of K_x/K_y is close to 0.5. Similar trends have been observed from analyses for other values of K_x/K_y. Separate charts are used to show behaviour in the velocity and acceleration-controlled conditions.

Response scenarios in the acceleration-controlled range tend to be more sensitive to the changes in the value of the eccentricity parameters resulting in higher edge displacement ratios compared to response scenarios in the velocity-controlled range.

The "stiff edge" of the building is the edge that is the closest to the CR whereas the flexible edge is furthest away from the CR. For cases where the value of b_r is greater than 1.0, the displacement ratio at the stiff edge is less than 1.0 meaning that displacements need to be checked at the flexible edge only. For this reason Figs. 8-11 presents edge displacement ratio for the flexible edge only.

The conditions of uni-axial asymmetry are represented by e_{yr}=0 on the design chart. Clearly, ignoring asymmetry in the direction of ground motion would always result in a conservative prediction of the edge displacement provided that the value of b_r is greater than 1.0. For the same reason estimates derived from analysis of uni-axial asymmetrical building models can be overly conservative when the buildings have large eccentricity in the (e_{yr}) direction.

It is cautioned herein that the displacement at both edges would need to be checked in cases where the values of b_r is equal to, or less than, 1.0 (refer Appendix for details).

It is also observed from Figs. 8-11 that building models with higher torsional stiffness (i.e., high b_r) are less sensitive to variations in the value of the eccentricity (in both the e_{xr} and e_{yr} direction).

In the seismic assessment of buildings, deformation in the weaker direction of the building can be more critical. Analyses have also been conducted on building models with stiffer perpendicular structural elements (K_x/K_y>1.0). Results for K_x/K_y of 2 are presented in Figs. 12-15. It is shown that the maximum displacement of buildings is less sensitive to the variations in the value of the eccentricity (in the e_{yr} direction) due to larger contribution of perpendicular elements to the torsional stiffness of the buildings. Ignoring the asymmetry in the perpendicular direction is shown to generally provide conservative estimates of the maximum displacement demand of the buildings.

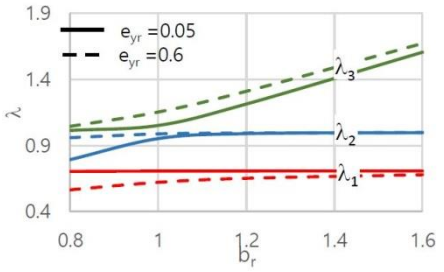

(a) e_{xr}=0.1

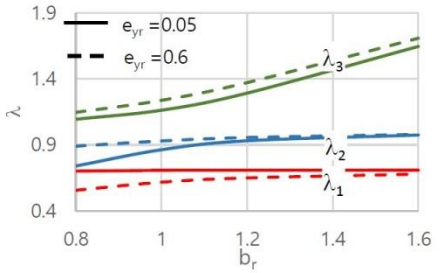

(b) e_{xr}=0.3

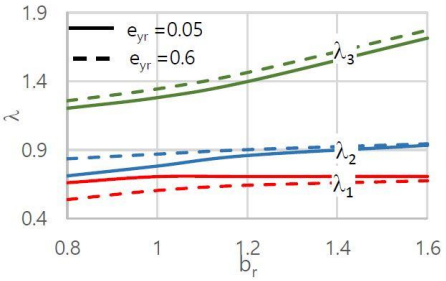

(c) e_{xr}=0.5

Fig. 7 Frequency ratios of the three coupled vibration modes

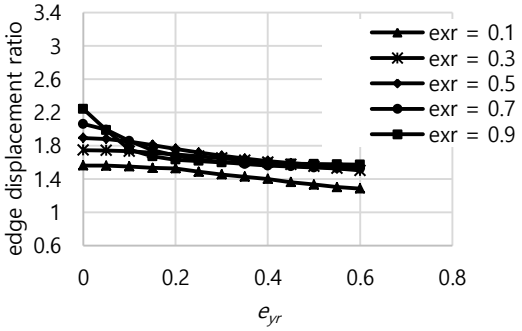

(a) Velocity-controlled range

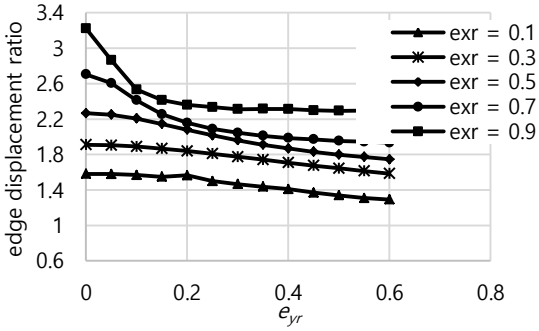

(b) Acceleration-controlled range

Fig. 8 Flexible edge displacement ratio of bi-axial asymmetric building models with b_r=1.1, K_x/K_y=0.5

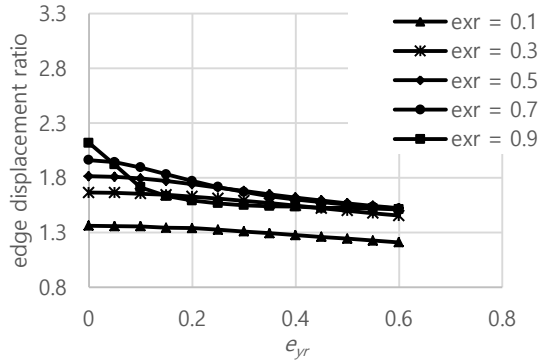

(a) Velocity-controlled range

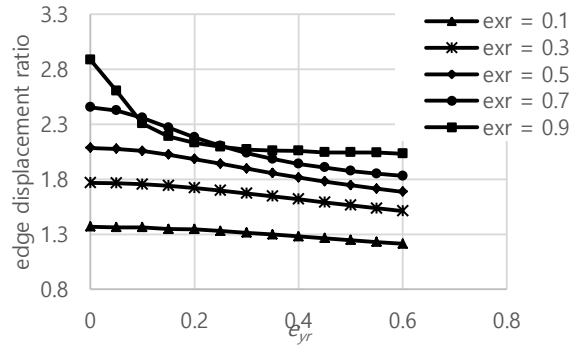

(b) Acceleration-controlled range

Fig. 9 Flexible edge displacement ratio of bi-axial asymmetric building models with b_r=1.2, K_x/K_y=0.5

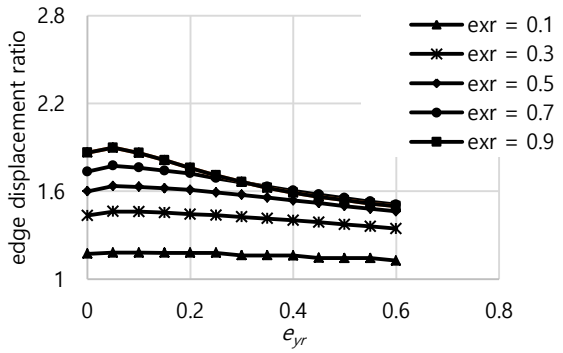

(a) Velocity-controlled range

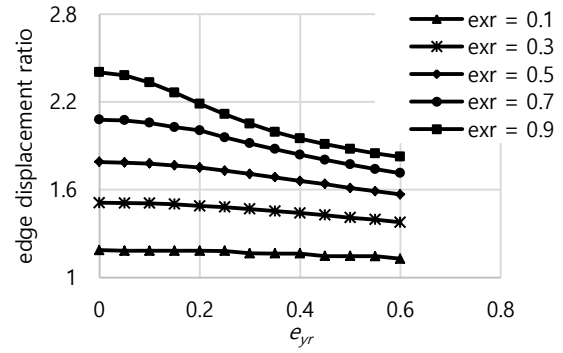

(b) Acceleration-controlled range

Fig. 10 Flexible edge displacement ratio of bi-axial asymmetric building models with b_r=1.4, K_x/K_y=0.5

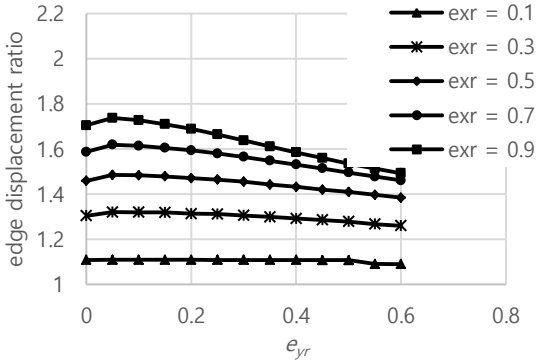

(a) Velocity-controlled range

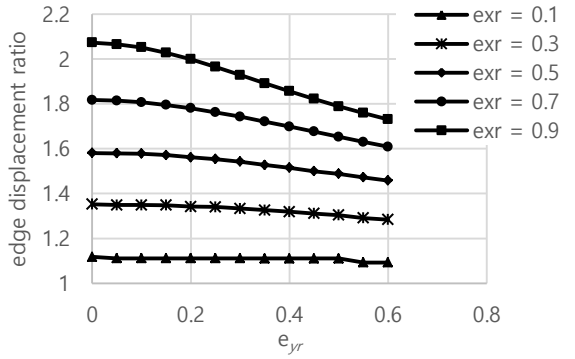

(b) Acceleration-controlled range

Fig. 11 Flexible edge displacement ratio of bi-axial asymmetric building models with b_r=1.6, K_x/K_y=0.5

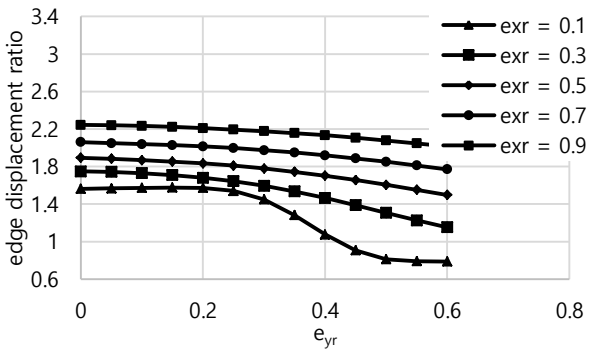

(a) Velocity-controlled range

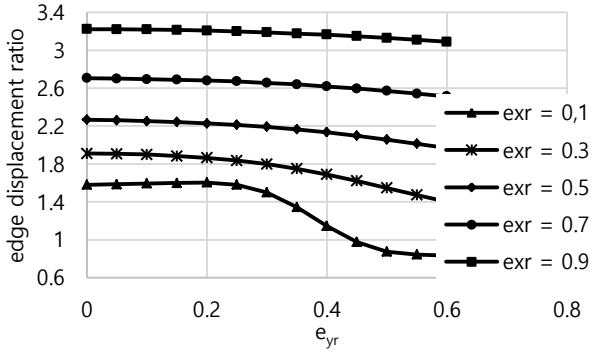

(b) Acceleration-controlled range

Fig. 12 Flexible edge displacement ratio of bi-axial asymmetric building models with b_r = 1.1, K_x/K_y = 2.0

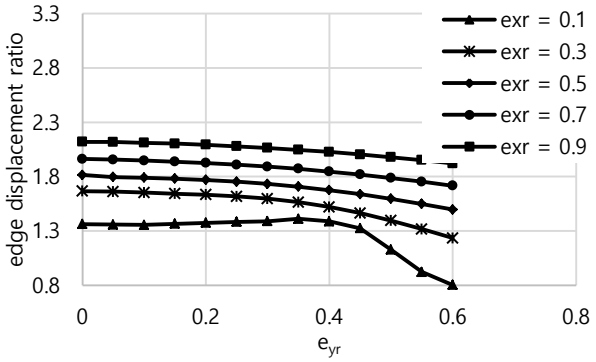

(a) Velocity-controlled range

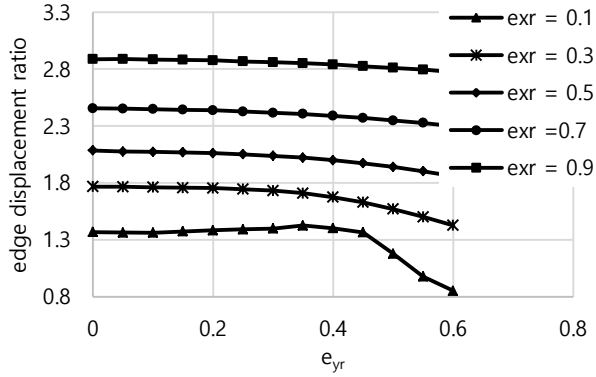

(b) Acceleration-controlled range

Fig. 13 Flexible edge displacement ratio of bi-axial asymmetric building models with b_r=1.2, K_x/K_y=2.0

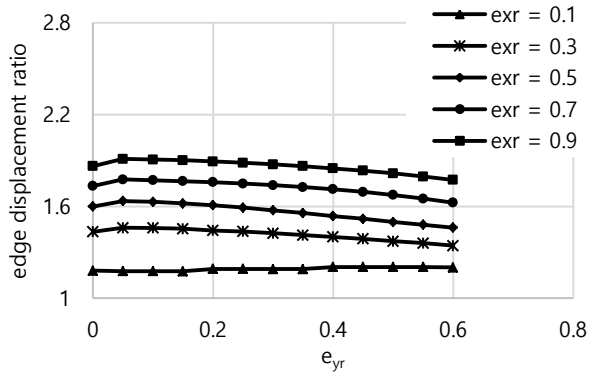

(a) Velocity-controlled range

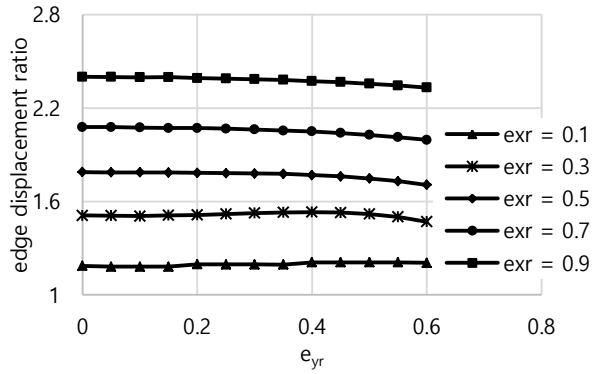

(b) Acceleration-controlled range

Fig. 14 Flexible edge displacement ratio of bi-axial asymmetric building models with b_r=1.4, K_x/K_y=2.0

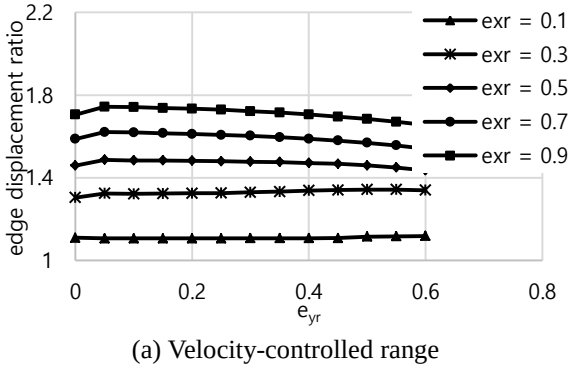

(a) Velocity-controlled range

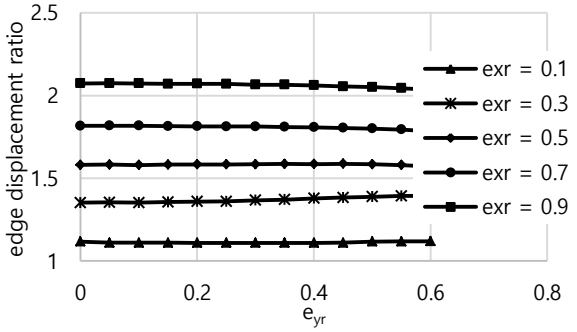

(b) Acceleration-controlled range

Fig. 15 Flexible edge displacement ratio of bi-axial asymmetric building models with b_r = 1.6, K_x/K_y = 2.0

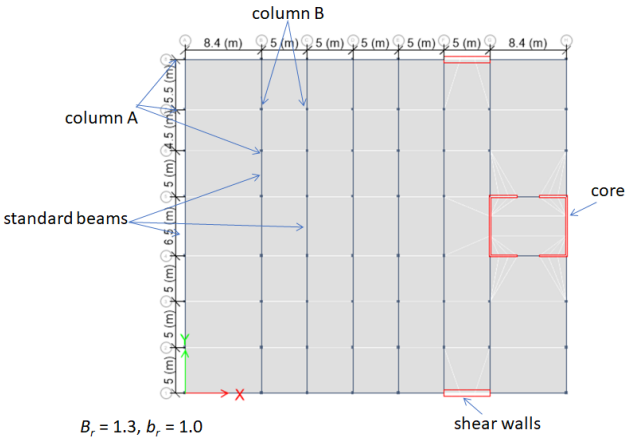

(a) Typical floor

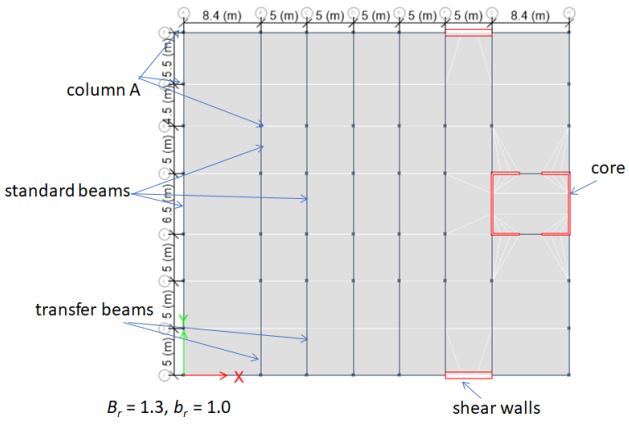

(b) Floor 2

Fig. 16 First example: Building 1 featuring uni-axial asymmetry

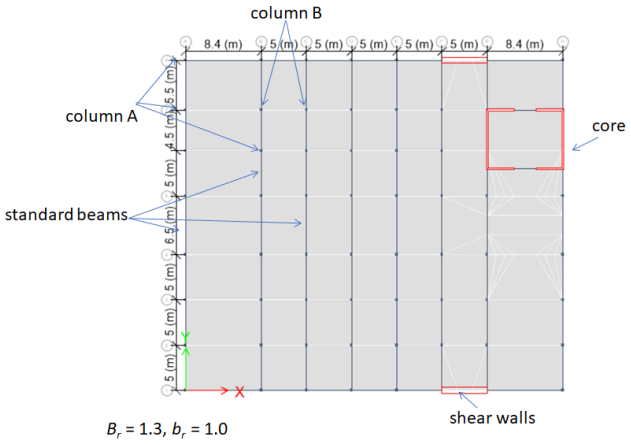

(a) Typical floor

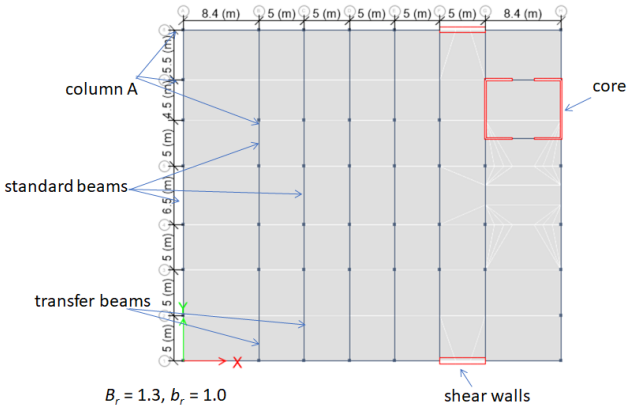

(b) Floor 2

Fig. 17 Second example: Building 2 featuring bi-axial asymmetry

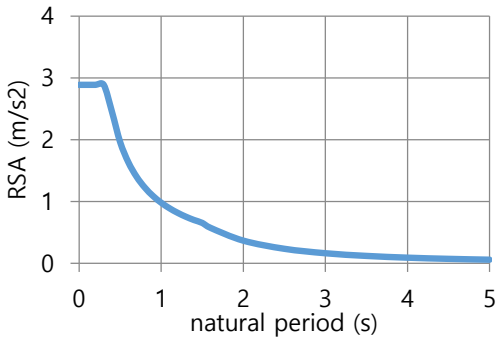

Fig. 18 Design response spectrum adopted for dynamic analyses (as per AS1170.4:2007)

Table 1 Dimensions of principal structural elements and material properties (mm)

(a) Building 1featuring uni-axial asymmetry

Element	Slab	Walls		Beams		Columns	
Type		Core	Shear	Standard	Transfer	A	B
Material	RC	RC	RC	RC	RC	RC	RC
Width (mm)	-	200	700	280	300	350	300
Depth (mm)	250	-	-	450	1600	350	300
Length (mm)	-			-	-		

(b) Building 2 featuring bi-axial asymmetry

Element	Slab	Walls		Beams		Columns	
Type		Core	Shear	Standard	Transfer	A	B
Material	RC	RC	RC	RC	RC	RC	RC
Width (mm)	-	200	650	280	300	350	300
Depth (mm)	250	-	-	450	1600	350	300
Length (mm)	-			-	-		

5. Comparison with results of multi-storey buildings

5.1 Description of the case study buildings

The practical application of the GFM methodology (Sections 2-4) is illustrated herein by working through two example six-storey reinforced concrete buildings which have been subject to 3D dynamic analyses for benchmarking purposes. The buildings were supported laterally by structural walls jointly with moment resisting frames (refer Figs. 16 and 17 for the floor plans). Some of the columns in the moment resisting frames featured discontinuity at the 2nd storey level. The 1st example building featured reinforced concrete walls that were asymmetrically disposed about the y-axis only thereby resulting in a TU framing system with uni-axial asymmetry. The 2nd example building featured asymmetry about both orthogonal axes, and the value of b_r remains to be the same as the 1st example. The ratio of the translational stiffness in the x-direction to the translational stiffness in the y-direction K_x/K_y is equal to 1.0.

The height of both buildings was 21.2 m. The inter-storey height is 4.2 m for the first and second storey and 3.2 m for the other storeys. The width of a typical floor plan was 41.8 m and mass radius gyration (r) was 16 m in order that the value B_r=1.3. The core walls (and shear walls) of both buildings were so configured to result in b_r=1.0. The geometric and material properties are presented in Table 1 whereas the mass and storey eccentricity of the individual floors are 10ehavior10e in Table 2. The modulus of elasticity and density of concrete was 24.5 GPa and 2500 kg/m^3 respectively.

Dynamic modal analyses of the buildings were conducted using program ETABS (Habibullah 1992) based on the use of the design response spectrum stipulated for 500 year return period earthquake as per AS1170.4:2007 for class *C* sites and a hazard factor of 0.08 g (Fig. 18). The fundamental natural period of vibration of both buildings was 0.52 s which is consistent with velocity-controlled conditions.

5.2 Applying the 10ehavior10ed force method of analysis (GFM)

First, planar 2D analysis was conducted on the building models ignoring plan asymmetry (refer Fig. 19 for the 2D view). The buildings were first subject to equivalent static analysis as per AS1170.4:2007. Values of the floor

Table 2 Storey mass and eccentricity

(a) Building 1 featuring uni-axial asymmetry

Level	Storey mass (t)	Eccentricity e_r	
		e_{yr}	e_{xr}
1	1287	0	0.91
2	1363	0	0.91
3	1241	0	0.89
4	1236	0	0.87
5	1236	0	0.86
roof	1171	0	0.88

(b) Building 2 featuring bi-axial asymmetry

Level	Storey mass (t)	Eccentricity e_r	
		e_{yr}	e_{xr}
1	1283	0.13	0.91
2	1356	0.16	0.91
3	1238	0.17	0.89
4	1233	0.19	0.87
5	1233	0.20	0.86
roof	1169	0.22	0.88

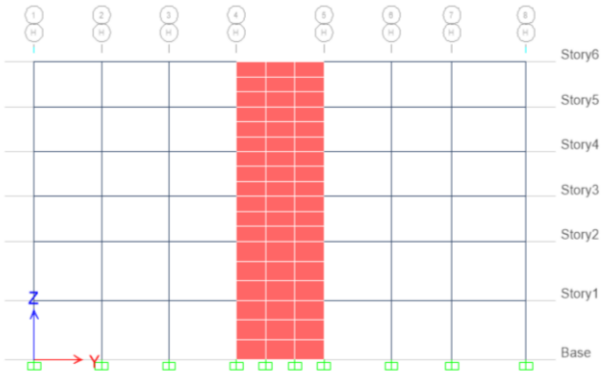

Fig. 19 2D view of the TU models

Table 3 Floor displacement values derived from equivalent static analysis as per AS1170.4:2007

Level	δ_i mm
Ground	0
1	0.9
2	2.3
3	3.6
4	5.0
5	6.4
Roof	7.7

displacement demands resulted from the application of lateral loads (totalling the base shear value) are listed in Table 3. Given that the geometry of both buildings were identical in elevation, the displacement demand behaviour as derived from 2D analysis of the buildings were also identical.

Given the floor displacement values of Table 3, parameter values of the single-degree-of-freedom (SDOF) idealisation can be calculated using Eqs. (1)-(3):

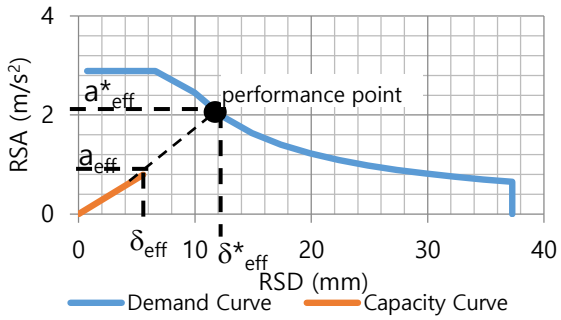

Fig. 20 The capacity and demand diagrams

Table 4 Displacement values based on the performance point

Level	δ_i mm	$\delta_i{}^* = \frac{\delta^*_{eff}}{\delta_{eff}}\delta_i$ mm	$F_i^* = \frac{\delta^*_{eff}}{\delta_{eff}}F_i$ kN	$V_i^* = \sum_i^n F_i^*$ kN
Ground	0	0		
1	0.9	2.0	537.6	11478.8
2	2.3	5.5	1158.0	10941.3
3	3.6	8.5	1625.1	9783.3
4	5.0	11.8	2113.2	8158.2
5	6.4	15.1	2856.4	6045.0
Roof	7.7	18.2	3188.6	3188.6

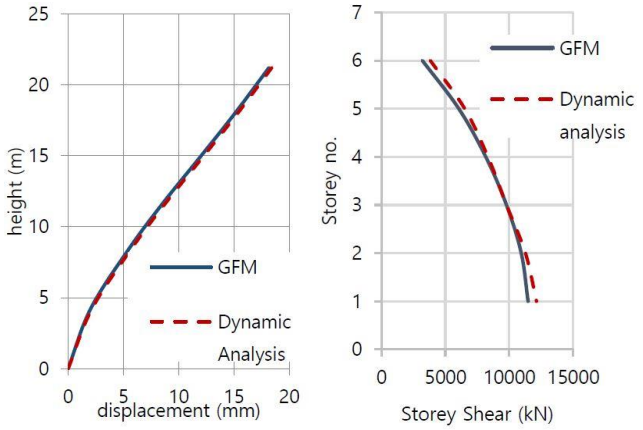

(a) Displacement (b) Storey shear

Fig. 21 Results from GFM and 2D dynamic analysis of TU building model

$\delta_{eff} = 5.8$ mm, $m_{eff} = 5618$ tonnes, $a_{eff} = 0.8\ m/s^2$

The capacity diagram was plotted and superimposed onto the demand diagram in the acceleration vs displacement (ADRS) diagram format (Fig. 20). The performance point as shown in the figure indicates an effective displacement $\boldsymbol{\delta_{eff}}^*$ value of 13 mm. The floor displacement and inertia force values were then scaled accordingly as shown in Table 4. Fig. 21 presents the comparison between the displacement and storey shear demand behaviour of the building as derived from the GFM and the 3D dynamic analysis of the building.

In order for the expressions for the amplification factors

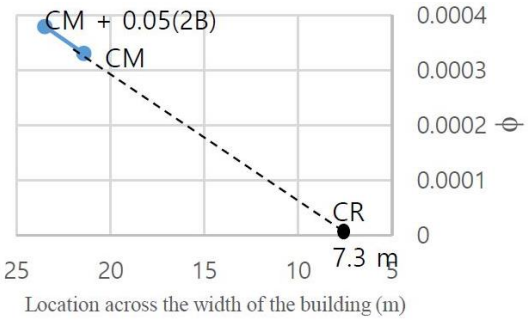

(a) rotation

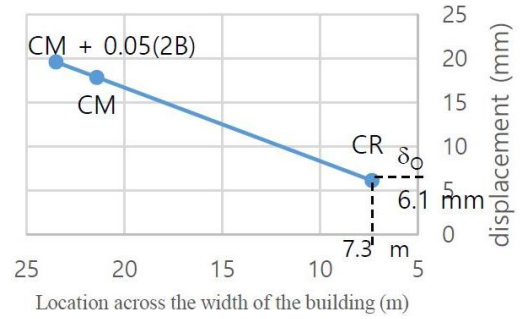

(b) displacement

Fig. 22 Correlation of rotation and edge displacement with location of the lateral load

derived in Sections 3 and 4 can be applied to the floor displacements to provide estimates of the maximum displacement demands of the TU multi-storey buildings, the multi-storey buildings were idealised into single-storey building models featuring plan asymmetry by following the method presented in Lam *et al.* (2016). The method requires determining the value of the eccentricity e_{xr} and that of the torsional stiffness parameter b_r noting that the dynamic torsional response behaviour of the building models are characterised by these two parameters. Detailed descriptions of the static analysis procedure for locating the CR of the building (hence value of e_{xr}) and determining the value of b_r can be found in Appendix C of Lam *et al.* (2016). To confirm the location of the CR a lateral load can be applied at the estimated location to ensure that building would not rotate on plan (refer Fig. 22(a)). The correlation of the edge displacement with the location of the lateral load as shown in Fig. 22(b) can be found from static analyses. The amount of edge displacement corresponding to applying lateral load at the location of the CR is the translational only displacement of the building (and is denoted herein as δ_0). The torsional stiffness parameter b_r can be inferred from information shown in Fig. 22(b) in conjunction with Eq. (24) which can be derived from the principles of statics (Lam *et al.* 2016).

$$\frac{\delta}{\delta_o} = 1 + \frac{e_r}{b_r^2}(e_r + B_r) \tag{24}$$

where, δ is the maximum displacement of the TU building subject to static lateral load applied at the CM, δ_o is the translational only displacement, e_r and b_r are the eccentricity and torsional stiffness parameter normalised with respect to the radius of gyration (r) and B_r is half of the width of the building normalised with respect to r.

Table 5 Torsional parameters of the two example buildings

		Eccentricity	
Building	b_r	e_{xr}	e_{yr}
1st example	1.0	0.89	0
2nd example	1.0	0.89	0.2

Table 6 Displacement values at the edges of 1st example TU building (featuring uni-axial asymmetry)

Level	$\boldsymbol{\delta_i}^*$ mm	$\delta_{stiff} = 0.6 \times \boldsymbol{\delta_i}^*$mm	$\delta_{flex} = 2.0 \times \boldsymbol{\delta_i}^*$mm
Ground	0.0	0.0	0.0
1	2.0	1.2	4.0
2	5.5	3.3	11.0
3	8.5	5.3	17.3
4	11.8	7.3	24.1
5	15.1	9.4	30.8
Roof	18.2	11.3	37.2

The process has to be repeated for the 2nd example TU building featuring bi-axial asymmetry for obtaining the value of eccentricity in the perpendicular direction (e_{yr}). Values of the eccentricity and torsional stiffness parameter for both example buildings are listed in Table 5.

In providing estimates for dynamic torsional actions Eqs. (9), (12) and (13b) were employed for calculating the values of the edge displacement ratio (δ/δ_o) for the stiff and flexible edges of the 1st example building (featuring uni-axial asymmetry). Values of the displacement ratio were calculated to be equal to 0.6 for the stiff edge and 2.0 for the flexible edge. The maximum displacement at the flexible and stiff edge were estimated by multiplying the translational displacement obtained from the planar two-dimensional analysis (Table 4) by the respective edge displacement ratio. The displacement values at the stiff and flexible edges of the TU building with uni-axial asymmetry are presented in Table 6. The maximum displacement values calculated for the edges of the TU building using the proposed GFM method can be verified by comparing against results from the 3D dynamic analysis of the building (Fig. 23). Close agreement between the two sets of results provide support for the use of GFM (which is essentially a static analysis procedure) for approximating results from 3D dynamic analysis of a building featuring uni-axial asymmetry.

The maximum displacement demand at the edges of the two example buildings (featuring uni-axial and bi-axial asymmetry) are compared in Fig. 24. Analysis of the uni-axial asymmetrical model is shown to provide conservative estimates of the edge displacement demand of the building consistent with the behavioural trends indicated in Figs. 8 – 11 in Section 4. Although the amount of difference displayed in Fig. 24 seems to be insignificant much greater differences are possible, and common.

Given the eccentricity and torsional parameters listed in Table 5 for the 2nd example (TU) building featuring bi-axial asymmetry the corresponding edge displacement ratio (δ/δ_o) can be found using Eqs. (20), (21), (22b) and (23b). The calculated values of δ/δ_o were 0.64 and 2.0 for the

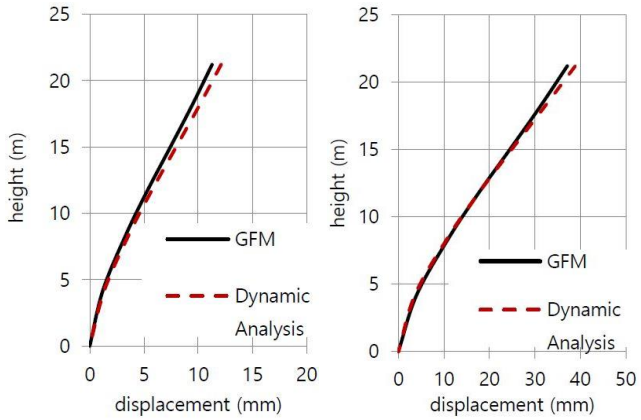

(a) Stiff edge (b) Flexible edge

Fig. 23 Displacement values obtained from GFM and 3D dynamic analysis of 1st example building featuring uni-axial asymmetry

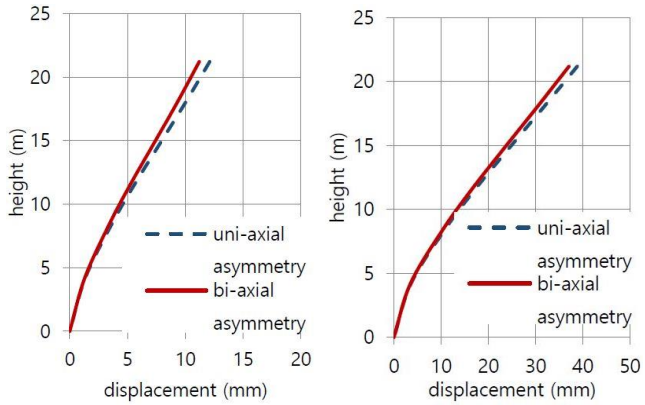

(a) Stiff edge (b) Flexible edge

Fig. 24 Edge displacement of uni-axial and bi-axial asymmetrical buildings

stiff and flexible edge, respectively. The maximum edge displacement values were obtained accordingly by multiplying the edge displacement ratio by the translational only displacement of a TB building (δ_o). These improved estimates of the edge displacement (by GFM) are compared against results from 3D dynamic analysis of the building (Fig. 25) showing close agreement. It is shown that that proposed method is able to provide reasonable estimates of the TU building with bi-axial asymmetry. The use of GFM (which is essentially a static analysis procedure) for approximating results from 3D dynamic analysis of a building featuring bi-axial asymmetry has been verified.

6. Conclusions

The current practice of placing reliance on the use of the computer to quantify design seismic actions is not entirely satisfactory given that no known calculation method exists to allow designers to independently evaluate results from the 3D dynamic analysis of a structure. Thus, static analysis has the intrinsic merit of allowing independent checks to be undertaken by a competent structural design engineer.

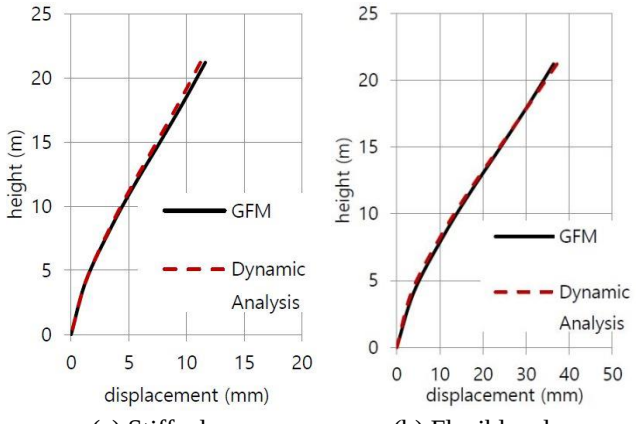

(a) Stiff edge (b) Flexible edge

Fig. 25 Displacement values obtained from GFM and 3D dynamic analysis of 2nd example building featuring bi-axial asymmetry

The Generalised Force Method (GFM) of analysis which is essentially a static analysis procedure is introduced to model the seismically induced displacement demand of low-rise, or medium-rise, buildings featuring uni-axial or bi-axial asymmetry based on the assumption of linear elastic behaviour. As the method is not intended for analysis of high-rise buildings (exceeding 30 m) the effects of the higher modes of vibration can be neglected. Algebraic expressions have been presented to provide estimates for the edge displacement ratio taking into account the effects of dynamic torsional actions. The expressions have been developed for buildings featuring uni-axial and bi-axial asymmetry. A parametric study conducted by varying torsional stiffness properties and eccentricity values in both directions indicate that buildings with high torsional stiffness are less sensitive to the variations in the value of the eccentricity in both directions. The uni-axial asymmetrical building models is shown to generally result in a conservative prediction of the edge displacement provided that the value of b_r is greater than 1.0. The maximum displacement of bi-axial asymmetrical building models is shown to be less sensitive to the variations in the value of the eccentricity in the perpendicular direction. Results generated by the use of GFM have been verified by comparison with results from 3D dynamic analyses of the building models.

Acknowledgments

The support of the Commonwealth Australia through the Cooperative Research Centre program and the University of Melbourne Early Career Researcher Grants Scheme is acknowledged.

References

Anagnostopoulos, S.A., Kyrkos, M.T. and Stathopoulos, K.G. (2015), "Earthquake induced torsion in buildings: critical review and state of the art", *Earthq. Struct.*, **8**(2), 305-377.

ASCE (2000), Prestandard and Commentary for the Seismic Rehabilitation of Buildings FEMA 356, Federal Emergency Management Agency, Washington, D.C., USA.

Building Seismic Safety Council (2003), NEHRP Recommended Provisions for Seismic Regulations for New Buildings and Other Structures Part I: Provisions (FEMA 450-1), Federal Emergency Management Agency; Washington, D.C., USA.

Ceci, A.M., Contento, A., Fanale, L., Galeota, D., Gattulli, V., Lepidi, M. and Potenza, F. (2010), "Structural performance of the historic and modern buildings of the University of L'Aquila during the seismic events of April 2009", *Eng. Struct.*, **32**(7), 1899-1924.

Chandler, A.M. and Duan, X.N. (1997), "Performance of asymmetric code-designed buildings for serviceability and ultimate limit states", *Earthq. Eng. Struct. Dyn.*, **26**, 717-735.

Chandler, A.M. and Hutchinson, G.L. (1986), "Torsional coupling effects in the earthquake response of asymmetric buildings", *Eng. Struct.*, **8**, 222-236.

Cimellaro, G.P., Giovine, T. and Lopez-Garcia, D. (2014) "Bi-directional pushover analysis of irregular structures", *J. Struct. Eng.*, **140**(9), 04014059.

D'Ambrisi, A., De Stefano, M. and Tanganelli, M. (2009), "Use of Pushover Analysis for Predicting Seismic Response of Irregular Buildings: A Case Study", *J. Earthq. Eng.*, **13**, 1089-1100.

Dempsey, K.M. and Tso, W.K. (1982), "An alternative path to seismic torsional provisions", *Soil Dyn. Earthq. Eng.*, **1**, 3-10.

Dimova, S.L. and Alashki, I. (2003), "Seismic design of symmetric structures for accidental torsion", *Bull. Earthq. Eng.*, **1**, 303-320.

EN 1998-1 (2004), Eurocode 8: Design of Structures for Earthquake Resistance – Part 1: General Rules, Seismic Actions and Rrules for Buildings, European Committee for Standardization, Brussels, Belgium.

Ferraioli, M. (2015), "Case study of seismic performance assessment of irregular RC buildings: hospital structure of Avezzano (L'Aquila, Italy)", *Earthq. Eng. Eng. Vib.*, **14**(1), 141-156.

Habibullah, A. (1992), ETABS Users Manual, Computers and Structures, Inc., Berkeley, California, USA.

Lam, N.T.K., Wilson, J.L. and Lumantarna, E. (2016), "Simplified elastic design checks for torsionally balanced and unbalanced low-medium rise buildings in lower seismicity regions", *Earthq. Struct.*, **11**(5), 741-777.

Lumantarna, E., Lam, N. and Wilson, J. (2013), "Displacement-controlled behavior of asymmetrical single-story building Models", *J. Earthq. Eng.*, **17**(6), 902-917.

Lumantarna, E., Mehdipanah, A., Lam, N. and Wilson, J. (2017), "Methods of structural analysis of buildings in regions of low to moderate seismicity", *The 2017 World Congress on Advances in Structural Engineering and Mechanics (ASEM17)*, Ilsan, Korea, August-September .

Magliulo, G., Maddaloni, G. and Cosenza, E. (2012), "Extension of N2 method to plan irregular buildings considering accidental eccentricity", *Soil Dyn. Earthq. Eng.*, **43**, 69-84.

Poursha, M., Khoshnoudian, F. and Moghadam, A.S. (2014), "The extended consecutive modal pushover procedure for estimating the seismic demands of two-way unsymmetric-plan tall buildings under influence of two horizontal components of ground motions", *Soil Dyn. Earthq. Eng.*, **63**, 162-173

Sommer, A. and Bachmann, H. (2005), "Seismic behavior of asymmetric RC wall buildings: principles and new deformation-based design method", *Earthq. Eng. Struct. Dyn.*, **34**(2), 101-124.

Standards Australia (2007), AS 1170.4-2007 Structural Design Actions-Part 4 Earthquake Actions, Standards Australia, Sydney, Australia.

Stathopoulos, K.G. and Anagnostopoulos, S.A. (2010), "Accidental design eccentricity: Is it important for the inelastic response of buildings to strong earthquakes?", *Soil Dyn. Earthq. Eng.*, **30**, 782-797.

Tscinias, T.G. and Hutchinson, G.L. (1981), "Evaluation of code requirements for the earthquake resistant design of torsionally coupled buildings", *Proc. Inst. Civ. Eng.*, **71**, 821-843.

Westenek, B., de la Llera, J. C., Jünemann, R., Hube, M. A., Besa, J. J., Lüders, C., ... and Jordán, R. (2013), "Analysis and interpretation of the seismic response of RC buildings in Concepción during the February 27, 2010, Chile earthquake", *Bull. Earthq. Eng.*, **11**(1), 69-91.

Wilson, J. and Lam, N. (2006), "Earthquake design of buildings in Australia using velocity and displacement principles", *Aust. J. Struct. Eng.*, **6**(2), 103-118.

Appendix

Figs. A1 and A2 present the edge displacement ratio for the stiff and flexible edges of bi-axial asymmetric building models with b_r values of 0.8 and 1.0.

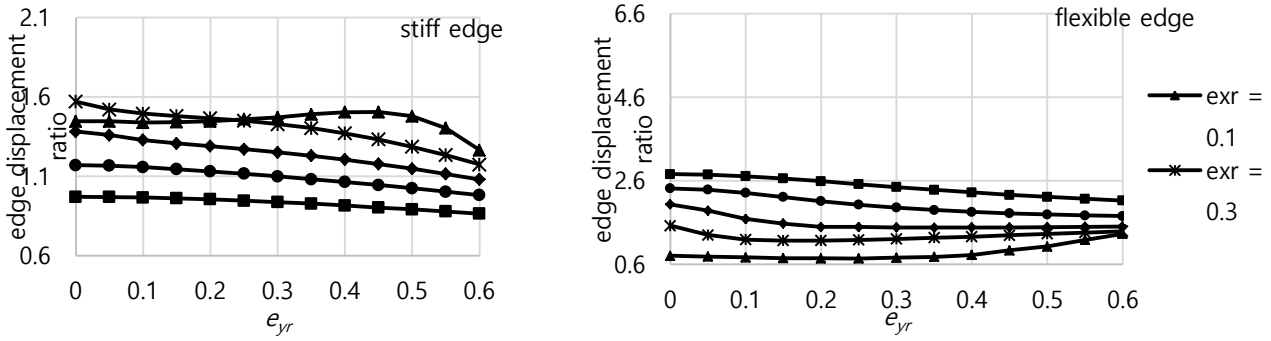

(a) Velocity-controlled range

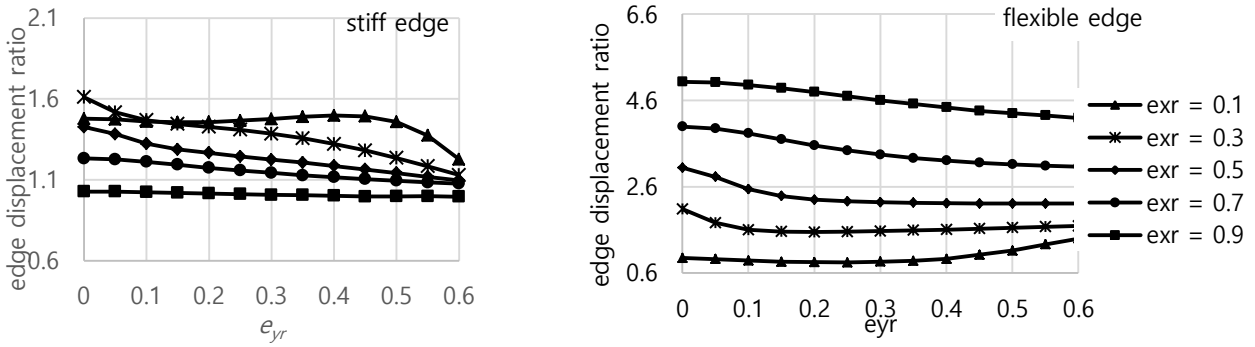

(b) Acceleration-controlled range

Fig. A1 Edge displacement ratio of bi-axial asymmetric building models with b_r=0.8, K_x/K_y=0.5

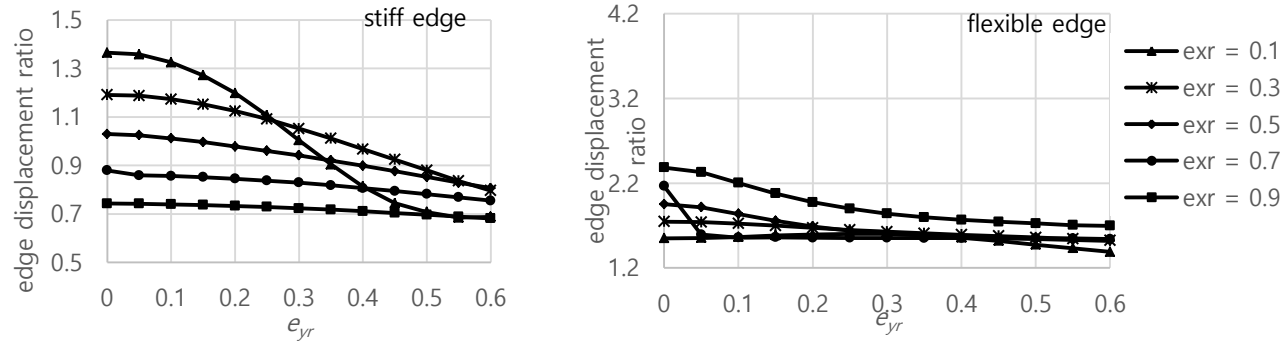

(a) Velocity-controlled range

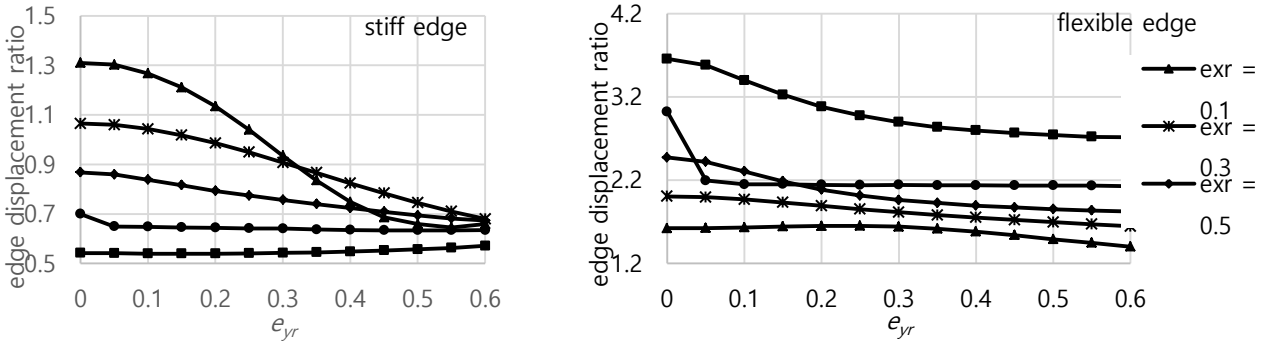

(b) Acceleration-controlled range

Fig. A2 Edge displacement ratio of bi-axial asymmetric building models with b_r=1.0, K_x/K_y=0.5